

# Abductive reasoning as the basis to reproduce expert criteria in ECG Atrial Fibrillation identification.

T Teijeiro, C A García, D Castro and P Félix

Centro Singular de Investigación en Tecnoloxías da Información (CiTIUS), University of Santiago de Compostela, Spain

E-mail: tomas.teijeiro@usc.es

**Abstract.** *Objective:* This work aims at providing a new method for the automatic detection of atrial fibrillation, other arrhythmia and noise on short single lead ECG signals, emphasizing the importance of the interpretability of the classification results. *Approach:* A morphological and rhythm description of the cardiac behavior is obtained by a knowledge-based interpretation of the signal using the *Construe* abductive framework. Then, a set of meaningful features are extracted for each individual heartbeat and as a summary of the full record. The feature distributions were used to elucidate the expert criteria underlying the labeling of the 2017 Physionet/CinC Challenge dataset, enabling a manual partial relabeling to improve the consistency of the classification rules. Finally, state-of-the-art machine learning methods are combined to provide an answer on the basis of the feature values. *Main results:* The proposal tied for the first place in the official stage of the Challenge, with a combined  $F_1$  score of 0.83, and was even improved in the follow-up stage to 0.85 with a significant simplification of the model. *Significance:* This approach demonstrates the potential of *Construe* to provide robust and valuable descriptions of temporal data even with significant amounts of noise and artifacts. Also, we discuss the importance of a consistent classification criteria in manually labeled training datasets, and the fundamental advantages of knowledge-based approaches to formalize and validate that criteria.

AMS classification scheme numbers: 68T10

*Keywords:* Abductive Reasoning, Atrial Fibrillation, ECG Processing, Arrhythmia Detection, 2017 Physionet Challenge

Submitted to: *Physiol. Meas.*

## 1. Introduction

In the last decades, the capacity of Artificial Intelligence to provide low-cost methods for the automatic diagnosis of cardiac diseases using standard ECG records has been a recurrent claim. There are thousands of works from many different approaches addressing various common problems, such as feature extraction, beat classification or rhythm analysis, among others (Sörnmo & Laguna 2005). Nevertheless, the potential shown in research results is still largely untapped in the clinical routine, and most of the current analysis tasks require an intensive intervention of expert clinicians. The Physionet/Computing in Cardiology Challenge tries every year to reduce this gap for some recognized problem, and in the 2017 edition it defied the scientific community and the industry to propose viable solutions to provide a reliable screening of Atrial Fibrillation from short single-lead ECG signals acquired with a commercial low-cost device (Clifford, Liu, Moody, Lehman, Silva, Li, Johnson & Mark 2017). A total of 8528 ECG records were provided as a training set, labeled in four classes: Normal sinus rhythm (**N**), Atrial fibrillation (**A**), Other rhythm (**O**) and Noisy ( $\sim$ ). A hidden test of 3658 records were used to evaluate the performance of the proposed algorithms, using as metric the mean  $F_1$  measure of the **N**, **A**, and **O** classes.

Besides pursuing a competitive numeric accuracy, the present work makes special emphasis on the interpretability of the results, as this has proven to be a major concern of care staff to trust automatic assistance methods (Caruana, Lou, Gehrke, Koch, Sturm & Elhadad 2015). For this, the classification procedure is based on a set of high-level features obtained from the description of the ECG in the same terms used by expert clinicians. This description is generated by the *Construe* algorithm (Teijeiro, Félix, Presedo & Castro 2016), which relies on abductive reasoning to obtain the best interpretation of the observed evidence, using a knowledge-based approach.

One of the main difficulties recognized by the participants in this Challenge is the absence of specific classification criteria beyond the name of each class. Even the expert clinicians labeling the training and test datasets received no instructions, leading to a large level of disagreement and many label inconsistencies (Clifford et al. 2017). Thus, machine learning methods hit a performance barrier that was below what it could be expected a priori. In our case, we tried to overcome this limit by elucidating the expert criteria underlying the training dataset and improving the label consistency according to that criteria, rather than tuning the learning algorithms. This strategy could even be improved in the follow-up stage of the Challenge, after a significant change of criteria between the training and test sets was unveiled in the data profile (Clifford et al. 2017).

The proposed classification algorithm is a combination of an abductive knowledge-based approach to interpret the raw signal with some learning-based methods that fit the decision parameters to the Challenge training set. Figure 1 shows the global architecture of the algorithm, that is described in detail in section 2 along with the manual data relabeling process. Afterwards, section 3 shows the validation results obtained on the Challenge training set and in the official and follow-up stages. Finally, section 4 discusses

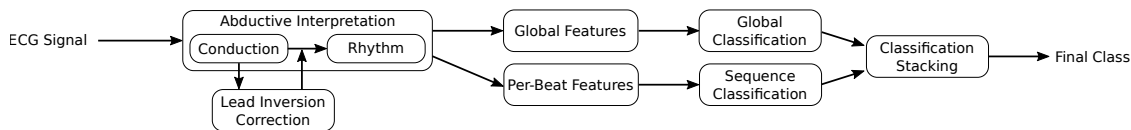


**Figure 1:** Algorithm architecture

these results, the potential of the proposed approach and a possible roadmap for the development of a low-cost automatic screening method for atrial fibrillation and other possible target arrhythmias.

## 2. Methods

### 2.1. Abductive interpretation of the ECG

The abductive interpretation of the ECG is the most distinguishing feature of our proposal. The result of this interpretation is a description in multiple abstraction levels of the physiological processes underlying the signal trace, in the same terms used by expert clinicians. Two abstraction levels are considered: the *conduction* level, that describes the signal as a sequence of P waves, QRS complexes and T waves, each with its corresponding morphology, amplitude and duration; and the *rhythm* level, that describes the signal as a concatenation of segments showing different rhythm patterns, including normal sinus rhythm, bradycardia, tachycardia, extrasystole, couplet, rhythm block, bigeminy, trigeminy, atrial fibrillation, ventricular flutter and asystole.

To build this description, the *Construe* algorithm implements a hypothesize-and-test cycle that pursues the best explanation of the observed evidence according to the available knowledge. The domain knowledge is defined as a set of *abstraction patterns* that describe the time and value constraints that have to be satisfied by evidence *observables* to support a given hypothesis. Abstraction patterns are dynamically generated from formal descriptions named *abstraction grammars*. The knowledge base for the interpretation of ECG signals is described in (Teijeiro et al. 2016).

The results of the abductive interpretation are also used to detect and fix possible inversions in the ECG signal. Lead inversion was found to be a quite common issue in the training set, affecting approximately 15% of the records. This is probably due to an incorrect holding of the acquisition device, and as a consequence it increases the chances to classify a record as abnormal due to the presence of infrequent QRS and T wave morphologies, as well as to the greater difficulty to identify the P waves.

This detection is performed from the *Construe* results at the conduction level and before carrying out the rhythm interpretation. The initial evidence are the beat annotations produced by the *gqrs* application from the Physionet library (Goldberger et al. 2000), from which a tentative delineation of the P wave, QRS complex and T wave of each heartbeat is obtained.

The inverted records were first identified manually, and then a simple logistic regression classifier was trained considering 14 features obtained from the raw signal

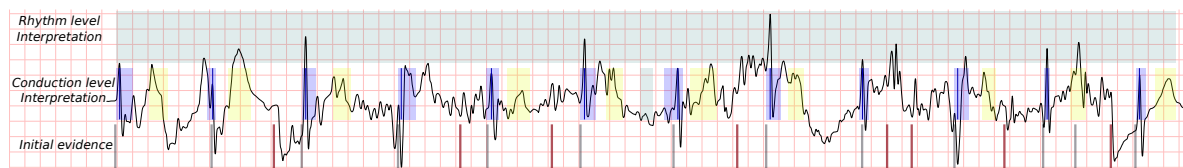


**Figure 2:** Fixing false positive detections. [Source: First 10 seconds of the A02080 record. Grey: Explained *gqrs* annotations. Red: Discarded *gqrs* annotations. Blue: QRS observations. Yellow: T wave observations. Green: P wave observation and Normal rhythm hypothesis.]

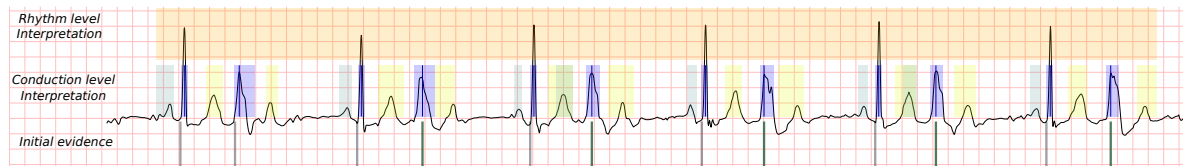


**Figure 3:** Fixing false negative detections. [Source: Record A01744 from second 4 to 14. Grey: Original *gqrs* annotations. Blue: QRS observations. Yellow: T wave observations and Bigeminy hypothesis. Green: Discovered beat annotations and P wave observations.]

and the delineation results. These features are 1) the median of the QRS axis; 2) the median of the QRS amplitude; 3) the difference between the mean and the median of the signal, normalized by the signal length and 4) by the signal amplitude; 5) the baseline value, calculated as the mode of the signal; 6) the ratio of the energy of the signal above and below the baseline; 7) the dispersion of the signal; 8) the mean value of the signal samples exceeding more than 3 standard deviations from the baseline; 9) the median amplitude of the first, 10) second, and 11) third waves inside the QRS complex; and the number of 12) P waves, 13) QRS complexes, and 14) T waves normalized by the signal length. The classifier showed a cross-validation F1 score of 0.96. If the signal is found to be inverted, all signal samples are multiplied by -1 before continuing.

After the lead inversion correction step, the *Construe* algorithm is executed up to the rhythm level taking as initial evidence the same set of QRS complexes used in the delineation step. This set can be modified during the interpretation process thanks to the non-monotonic reasoning scheme that combines bottom-up reasoning (guided by data) and top-down reasoning (guided by knowledge) to obtain the best matching between observations and knowledge. This gives great robustness to the presence of noise and artifacts in the ECG data, and allows to fix both false positive and false negative QRS detections, as shown in Figures 2 and 3. In Figure 2, the high amount of noise in the signal causes many false positive beat detections, that are fixed at the rhythm level by selecting as the best explaining hypothesis a single normal rhythm observation. In Figure 3, all but the first ventricular beat are not detected, probably due to the lower amplitude and slope. Still, the bigeminy hypothesis evoked by the first extrasystole allows to look for further advanced beats, explaining the full fragment with this rhythm hypothesis.

## 2.2. High level feature extraction

The description resulting from the abductive interpretation stage contains the information typically referred by expert clinicians and ECG handbooks to make a decision about the normal/abnormal condition of a record. However, since the criteria leading to each label is not provided, this information is converted to a set of quantitative features that will be the input for two selected machine learning methods in order to fit the underlying criteria of the training set. One of the methods evaluates each record globally, using aggregated features; while the other evaluates the record as a sequence, using a Recurrent Neural Network architecture fed with individual features for each detected heartbeat. These two methods are detailed below.

In the proposal submitted to the official phase of the Challenge (Teijeiro, García, Castro & Félix 2017), a total of 79 features were calculated. Yet, the final results obtained in the test set showed a significant overfitting of the training set, which is a sign of an excessive complexity of the model. Thus, in the new version the set of global features was reduced using the Recursive Feature Elimination technique (Guyon, Weston, Barnhill & Vapnik 2002), resulting in 42 features that are detailed in Table 1. Two of these features, `RR_Irr` and `RR_MIrr`, were not included in the previous version and correspond to a rhythm irregularity measure based on sample entropy estimation, which is described in (Petrenas, Marozas & Sörnmo 2015).

Some of these features require further explanation. Specifically, the term *profile* refers to the sum of the absolute value of the derivative signal, and is an excellent signal quality indicator. Regarding `Pdistd` and `MPdist`, the referred measure corresponds to the distance to the separating hyperplane of the one class SVM used by *Construe* to perform the delineation of P waves, and intuitively it is a measure of “how much it really looks like a P wave”.

Most of the individual features used to train the sequence classifier described in section 2.5 are just disaggregations of the features in Table 1, such as `RR`, `RR_Irr`, `n_PR`, `prof`, `pw_prof`, `Pdist`, `QT`, `TP` and `TP_freq`. Additionally, various morphological features were added to enable the identification of isolated conduction alterations. These features include the duration, amplitude and turning point of each individual wave inside the QRS complex, the QRS axis, the P and T waves duration and amplitude, and the ST segment deviation. Also, two qualitative features were included to describe the QRS morphology tag (*qRs*, *QS*, *rSr'*, etc.) (Teijeiro, Félix & Presedo 2015) and the name of the rhythm in which the heartbeat was interpreted.

## 2.3. Expert criteria elucidation and data relabeling

Every non-random human labeling task has a set of underlying criteria. These criteria may be subtle, unconscious, or even variable along time, but they necessary exist. The objective of any machine-learning algorithm trying to reproduce this labeling will therefore be to formalize and quantify these underlying criteria, and in consequence, the more formalized these criteria are a priori, the easier will be the development of

**Table 1:** Set of features used to train the global classifier

<b>tSR:</b> Proportion of the record length interpreted as a regular rhythm (Normal rhythm, tachycardia or bradycardia).	<b>t1b:</b> Number of milliseconds from the beginning of the record to the first interpreted heartbeat.
<b>tOR:</b> Number of milliseconds interpreted as a non-regular rhythm.	<b>longTch:</b> Longest period of time with heart rate over 100bpm.
<b>RR:</b> Median RR interval of regular rhythms.	<b>RRd_std:</b> Standard deviation of the instant RR variation.
<b>RRd:</b> Median Absolute Deviation (MAD) of the RR interval in regular rhythms.	<b>MRRd:</b> Max. absolute variation of the RR interval in regular rhythms.
<b>RR_MIrr:</b> Max. RR irregularity measure.	<b>RR_Irr:</b> Median RR irregularity measure.
<b>PNN{10,50,100}:</b> Global PNNx measures.	<b>o_PNN50:</b> PNN50 of non-regular rhythms.
<b>mRR:</b> Min. RR interval of regular rhythms.	<b>o_mRR:</b> Min. RR interval of non-regular rhythms.
<b>n_nP:</b> Proportion of heartbeats with detected P-wave inside regular rhythms.	<b>n_aT:</b> Median of the amplitude of the T waves inside regular rhythms.
<b>n_PR:</b> Median PR duration inside regular rhythms.	<b>Psmooth:</b> Median of the ratio between the standard deviation and the mean value of P-waves' derivative signal.
<b>Pdistd:</b> MAD of the measure given by the P wave delineation method.	<b>MPdist:</b> Max. of the measure given by the P wave delineation method.
<b>prof:</b> Profile of the full signal.	<b>pw_prof:</b> MAD of <b>pw_prof</b> .
<b>xcorr:</b> Median of the maximum cross-correlation between QRS complexes interpreted in regular rhythms.	<b>o_xcorr:</b> Median of the maximum cross-correlation between QRS complexes interpreted in non-regular rhythms.
<b>PRd:</b> Global MAD of the PR durations.	<b>QT:</b> Median of the corrected QT measure.
<b>TP:</b> Median of the prevailing frequency in the TP intervals.	<b>TPfreq:</b> Median of the frequency entropy in the TP intervals.
<b>pw_prof:</b> Profile measure of the signal in the P-wave area.	<b>nT:</b> Proportion of QRS complexes with detected T waves.
<b>n_Txcorr:</b> Median of the maximum cross-correlation between T-waves inside regular rhythms.	<b>n_Pxcorr:</b> Median of the maximum cross-correlation between P-waves inside regular rhythms.
<b>baseline:</b> Profile of the baseline in regular rhythms.	<b>o_baseline:</b> Profile of the baseline in non-regular rhythms.
<b>wQRS:</b> Proportion of wide QRS complexes (duration longer than 110ms).	<b>wQRS_xc:</b> Median of the maximum cross-correlation between wide QRS complexes.
<b>wQRS_prof:</b> Median of the signal profile in the 300ms before each wide QRS complex.	<b>w_PR:</b> Proportion of heartbeats with long PR interval (longer than 210 ms).
<b>x_xc:</b> Median of the maximum cross-correlation between ectopic beats.	<b>x_rrel:</b> Median of the ratio between the previous and next RR intervals for each ectopic beat.

such an algorithm. Probably, the most labor-intensive task of our proposal was the elucidation of the expert criteria underlying the training and test sets, and the ensuing data relabeling to make these criteria as consistent as possible along the dataset.

Certainly, the most difficult class to define an appropriate discrimination knowledge is the **O** class, inasmuch as the only provided information (the class name) is excessively vague and it may include a range of pathophysiological processes showing very different morphologies and rhythms. Hence, since this class is opposed to atrial fibrillation and normal sinus rhythm, one expert may consider that only rhythm alterations should be included in this class, while another expert may contemplate any event that is out of normality, such as conduction delays or chamber enlargements, among others.

Thanks to the physiological meaning of the features provided by the interpretation, it has been possible to throw light on some well-known ECG alterations that seem to be considered as **O** representatives in the training set. A simple but valuable tool is the per-class distribution of each feature. Figure 4 shows the distributions of three features

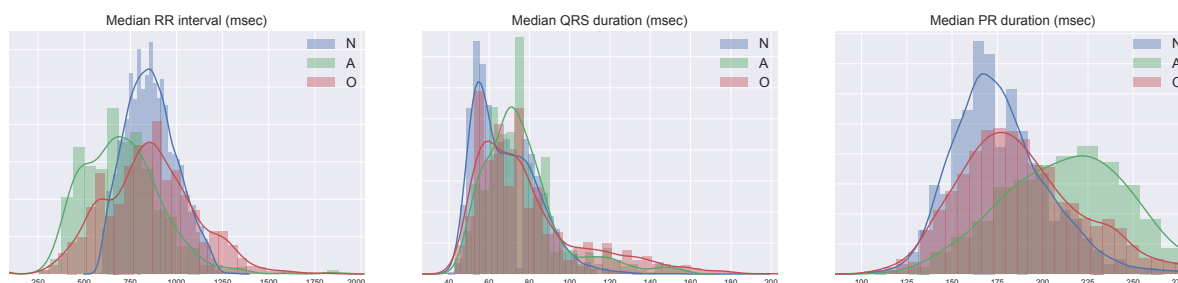
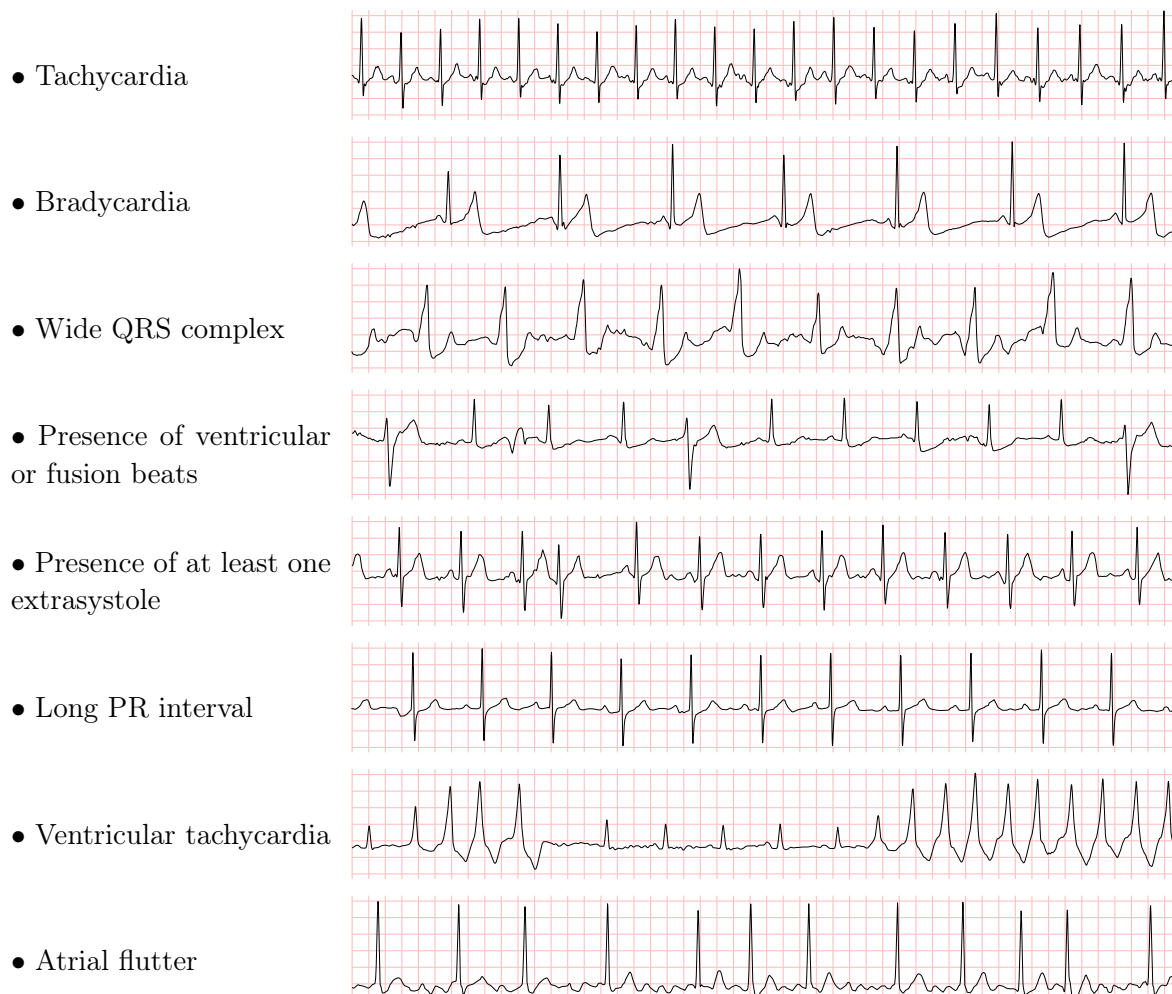


**Figure 4:** Per-class distribution of three representative features (best seen in color).

that define an almost crisp threshold for some well-known anomalies. It can be seen that the tachycardia and bradycardia abnormal rhythms are considered to have a median RR interval below 600ms and over 1200ms, approximately. Also, a QRS complex wider than 110ms seems a clear indicator of anomaly, and a PR duration over 220ms also has a bias to the **O** class with respect to **N**, although in this case the separation is less clear-cut.

Using this procedure, the following recognized rhythm and conduction conditions were identified to be labeled as **O** in the training set (a representative record of each anomaly is also displayed, corresponding to **A07833**, **A05308**, **A06071**, **A00688**, **A05301**, **A06295**, **A00741** and **A00326** records):



Each of these conditions is sufficient to classify a record as **O** in many cases, such as those shown above. However, these criteria are not consistent across the entire dataset and there are examples of these phenomena in several classes. Some examples are shown in Figure 5.

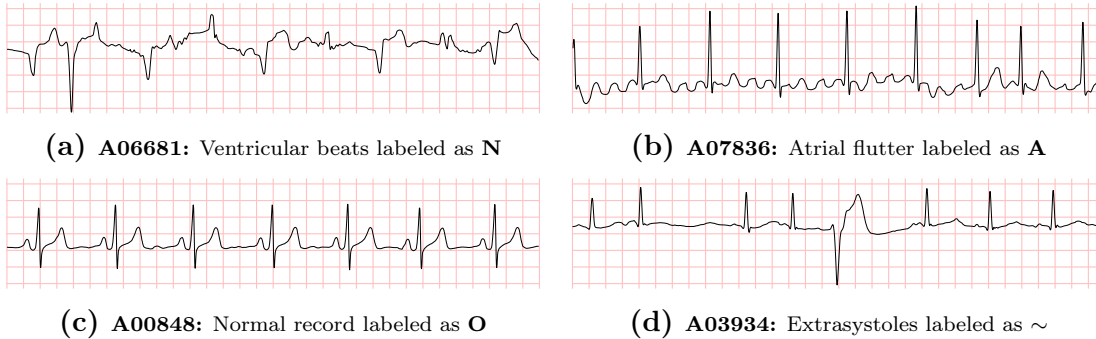


**Figure 5:** Inconsistent labels in the training set

Inconsistencies seriously undermine the performance of machine learning algorithms, inasmuch as trying to fit arbitrary decisions lead to more complex and overfitted models. Hence, a partial manual relabeling process guided by misclassified examples was performed for the official phase of the Challenge. This process tried to be conservative and focused on clear examples of the abovementioned anomalies that were not labeled as **O**. A total number of 197 out of 8528 records were relabeled in this stage, named V2.

During the official phase, a significant portion of the records in the hidden test set was relabeled by up to eight human experts, following a bootstrap approach based on the disagreement level of the top scored algorithms. Some basic statistics about this process were published by the organizers (Clifford et al. 2017, Table 2), showing an important reduction of the records labeled as **O**, with a relative decrease of about 33%. This suggest a significant change of the underlying classification criteria, being more conservative towards the **N** and  $\sim$  classes. Since labels in the training set were not modified accordingly, cross-validation was no longer a reliable predictor of the performance of the algorithms in the test set, and intuition became much more relevant.

Following this intuition, a second relabeling stage was performed for the follow-up phase of the Challenge. It is reasonable to think that the change of criteria in favor of the Normal and Noise classes had a greater impact on records showing a regular sinus rhythm, so the conduction criteria (wide QRS complex and long PR interval) were no longer considered sufficient for the **O** class. Also, and taking into account that the signal was captured by subjects participating actively and with a handheld device, phenomena like ventricular tachycardias were considered implausible, and patterns like those appearing in record A00741 were labeled as noise. A total number of 747 records were relabeled in this stage, named V3. Table 2 shows a comparison of the class distributions in the training set before and after relabeling for each phase of the challenge, and the distribution in the hidden test set.

**Table 2:** Class distribution before/after manual relabeling

Class	Official V2	Relabeled V2	Official V3	Relabeled V3	Test Set
<b>N</b>	59.2%	57.4%	59.5%	64.8%	66.6%
<b>A</b>	8.7%	8.6%	8.9%	8.6%	7.8%
<b>O</b>	28.8%	30.7%	28.3%	23.0%	18.7%
$\sim$	3.3%	3.2%	3.3%	3.6%	6.9%

Additionally, the heuristics guiding the *Construe* algorithm were slightly modified to encourage normal rhythm hypotheses. Specifically, if a signal fragment shows evidence compatible with the presence of QRS complexes at regular intervals and with a frequency between 50 and 110 beats per minute, then the fragment is considered fully explained and no other rhythm hypotheses are explored. This adjustment can potentially ignore important anomalies such as interpolated extrasystoles, but it was observed that with a single lead it is infeasible to morphologically distinguish many artifact patterns from real ectopic QRS complexes, so the simplicity principle is enforced in this case.

#### 2.4. Global classification

As shown in Figure 1, the label for a given record is obtained by combining two different classification algorithms. The first one is a “global” classifier, that makes a decision based on a summary information of the full record. It is defined as a standard multilabel classifier  $\mathcal{F} : \mathcal{X} \rightarrow \mathcal{Y}$ , where  $\mathcal{X}$  is the feature space defined in Table 1 and  $\mathcal{Y} = \{\mathbf{N}, \mathbf{A}, \mathbf{O}, \sim\}$ .

The selected machine learning method was the Tree Gradient Boosting algorithm, and particularly the XGBoost implementation (Chen & Guestrin 2016), which achieved significantly better results than other state-of-the-art methods such as Support Vector Machines or Random Forests without any hyperparameter tuning. Also, this algorithm provides a certain degree of interpretability by assigning different importances to the classification features. Table 3 shows a basic comparison of the  $F_1$  score obtained for each class and for the final metric by each of these algorithms on the training set after relabeling, using 200-fold cross-validation. For SVM and Random Forest, the scikit-learn v0.18 implementation was used (Pedregosa, Varoquaux, Gramfort, Michel, Thirion, Grisel, Blondel, Prettenhofer, Weiss, Dubourg, Vanderplas, Passos, Cournapeau, Brucher, Perrot & Duchesnay 2011).

**Table 3:** Algorithm comparison for global classification without hyperparameter tuning

	SVM	Random Forest	XGBoost
<b>N</b>	0.95	0.95	0.96
<b>A</b>	0.80	0.77	0.81
<b>O</b>	0.81	0.82	0.86
$\sim$	0.67	0.63	0.69
<b>Overall</b>	<b>0.85</b>	<b>0.85</b>	<b>0.88</b>

Hyperparameter tuning for XGBoost was performed using exhaustive grid search and 8-fold cross-validation. The tested and selected values are shown in Table 4.

**Table 4:** Hyperparameters tested for XGBoost optimization

Maximum tree depth: <b>5</b> , 6, 7, 10 and 12.	Gamma: 0.2, 0.4, 1.0 and <b>2.0</b> .
Learning rate: <b>0.1</b> , 0.2 and 0.4.	Subsample: <b>0.8</b> , 0.9 and 1.0.
Number of boosting rounds: 25, 50, 75 and <b>100</b> .	Min. child weight: 5, <b>7</b> , 10 and 15.

The obtained results gave a best mean  $F_1$  score of  $0.886 \pm 0.015$ . The worst result was  $0.858 \pm 0.008$ , but more than 90% of the hyperparameter combinations were within the standard deviation of the best result, that is, over 0.871. As the variability is so low, we decided to choose conservative values for most of the hyperparameters to build a more general model. The selected values are highlighted in bold, and gave a score of  $0.883 \pm 0.010$ . On the training set, the global classifier achieved a score of 0.942.

### 2.5. Sequence classification

The second classification algorithm shown in Figure 1 was conceived as a complement to the global classifier, by working in a beat-by-beat basis instead of dealing with features summarizing the whole record. Consider, for example, an almost normal record with just an ectopic beat. Unless the summary of the record and the global classifier are extremely accurate, these type of records will probably be misclassified. However, a classifier specialized in processing sequences of beats could correctly classify the record by remembering that an abnormal heartbeat has occurred. There is another compelling reason for using a sequence classifier. Although *Construe* is able to extract meaningful features in noisy segments, it is reasonable to give more credence to clean measurements than to noisy ones. Unlike with global features, this is easy to achieve with the sequence classifier, in which each heartbeat receives its own signal quality indicator.

The need for remembering the occurrence of (probable) distant events led us to use Long Short Term Memory networks (LSTMs) as the basis of the sequence classifier. The key idea behind LSTMs is the use of a cell memory which can store useful information over time, and several non-linear gating units that decide which information should be added and removed from the cell. The use of the gating cells is also important to avoid vanishing or exploding gradients, an important issue when backpropagating through time and which may prevent the network from learning long-range dependencies.

The architecture of the sequence classifier is shown in Figure 6. At each time step the features associated with a single heartbeat are transformed using a time-distributed multilayer perceptron (MLP). The purpose of the MLP is to find a transformation of the input features into a new embedding space with easier temporal dynamics. The MLP consists of 256 hidden units followed by a Rectifier Linear Unit (ReLU) (Glorot, Bordes & Bengio 2011) which maps the input features into a 128 dimensional output space. The *LSTM\_0* network further processes the sequence of transformed heartbeat features and

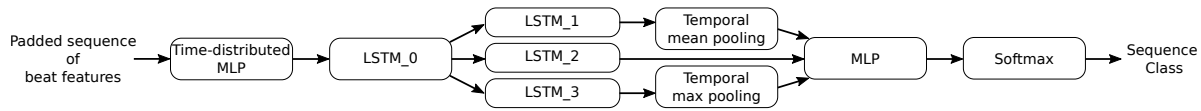


**Figure 6:** The sequence classifier based on LSTMs.

outputs another sequence that is used as input for the remaining LSTMs. The  $LSTM\_2$  only returns the final state of the network, which is subsequently used to output the final classification label. Therefore, the central processing pipe of Figure 6 may be seen as a stacked LSTM model, which is widely used in machine learning tasks. The processing pipes that involve the  $LSTM\_1$  and  $LSTM\_3$  networks require further explanation. Both LSTMs return new sequences that are transformed into feature vectors by using a pooling operation that drops its temporal dimension. The mean pooling averages the outputs of the  $LSTM\_1$  across its temporal dimension, whereas that the max pooling picks the maximum values of each dimension of the  $LSTM\_3$  outputs. Intuitively, what we are trying to achieve with these operations is to simulate the reasoning of clinicians that, after seeing a complete record, look for some extreme events (the max pooling operation) or for some subtle event that occurs during the whole record (mean pooling). All the LSTMs used a hidden state of 128 units. Finally, another MLP with 256 hidden units and ReLU activation concatenates and processes the outputs of the LSTMs before a Softmax layer, which predicts a probability for each of the 4 classes.

The proposed model has a large amount of degrees of freedom and therefore, preventing overfitting was a major concern.  $L^2$ -regularization was applied to all layers of the model, using a regularization strength of  $10^{-4}$ . Dropout was also applied to improve generalization. This is achieved by randomly turning off several neural units during training, which prevents feature co-adaptation. That is, each neural unit becomes more robust since during training time it cannot rely on other units to correct its mistakes (Srivastava, Hinton, Krizhevsky, Sutskever & Salakhutdinov 2014). The amount of dropout was different for each layer of the model: The MLP layers used 0.25,  $LSTM\_0$  used 0.22 for its inputs and 0.44 for its recurrent states, and the remaining LSTMs used 0.35 for its inputs and 0.36 for its recurrent states. Early stopping was also employed, ending the training after 15 epochs without improvement on a validation set obtained from a stratified random 85:15 split. The use of early stopping implies that a small fraction of the data would not be used for training the neural network. To use all the available data, 3 sequence classifiers were trained using 3 different validation sets. We limited the number of LSTMs to 3 to avoid exceeding the Challenge entry size limit. The final prediction of the sequence classifier is obtained by averaging the predictions of each of the 3 classifiers. Besides using all the available data, averaging different models helps in reducing the variance that results from the random initialization of the neural network layers and the random split between training and validation set. Averaging similar models is also known to reduce overfitting. In this sense, this averaging may be seen as a very simple sub-bagging.

The sequence classifier was trained by using the categorical cross-entropy as the loss function, a batch size of 32 records, and Adam as optimizer (Kingma & Ba 2014). The initial learning rate of the optimizer was set to 0.002, The use of a train and a validation set also permitted us to monitor the performance of the classifier and to decrease the learning rate when the validation loss was stacked in a plateau. The learning rate was decreased by a factor of  $\sqrt{2}$  after 3 epochs without improvement.

All the hyperparameters previously discussed were selected by using a tree of Parzen estimators, an hyperparameter optimization algorithm based on approximating the performance of the hyperparameters by using Bayesian modeling (Bergstra, Yamins & Cox 2013). The sequence classifier was implemented using Keras (Chollet et al. 2015).

### 2.6. Classifier stacking

The global and sequence classifiers were blended together by means of the stacking technique. Stacking (or stacked generalization) is an ensemble learning method that combines several classifiers by using another meta-classifier (Wolpert 1992). Stacked classifiers usually achieve better performance than the base classifiers by using each level 0 model where it performs best. Therefore, the level 0 classifiers should be diverse enough so that they may complement each other when combined. Furthermore, the more each classifier has to say about the data, the better the resultant stacked classifier (Wolpert 1992). In our approach, both requirements are fulfilled. A Linear Discriminant Analysis (LDA) was chosen as meta-classifier. The inputs of the LDA are the predicted probabilities from each of the level 0 classifiers. However, to avoid possible collinearity issues, only 3 probabilities from each model are used. An important point to keep in mind when training stacked classifiers is that it requires a partition of the dataset. If we fitted the level 0 classifiers using all data, then the second meta-classifier will be biased towards the best of the two models. Algorithm 1 describes how we implemented the partitions required by both the sequence classifier and the stacking classifier.

## 3. Results

Tables 5 and 6 show the validation results of the classification algorithms in the public and hidden Challenge datasets. Table 5 shows how the stacking technique usually improves the performance of the individual classifiers, achieving a better mean score with lower variance. Table 6 shows the same results but disaggregated for each target class, where we can see that the magnitude of the improvement is almost equal for all classes. Also, Table 6 shows the improvement obtained in the follow-up stage of the Challenge with respect to the official phase, confirming the change of criteria introduced in the bootstrap relabeling and the importance of label consistency. Yet, the notable performance decrease in the hidden test set with respect to cross-validation suggest that there are still criteria differences between the training and test sets.

---

**Algorithm 1** algorithm for the stacking classifier. In our implementation we use  $n\_nets=3$ .

---

**INPUT:** The *data* consisting on the *Construe* features and the classification labels, and the number of neural nets to train  $n\_nets$

**function** TRAINLSTMS(train\_data)

    splits = STRATIFIEDSPLIT(train\_data, n\_splits=n\_nets, size=0.15)

    lstms = {TRAINLSTM(train, validation) | train, validation  $\in$  splits}

**return** lstms

**end function**

metafeatures =  $\emptyset$   $\triangleright$  Probability predictions of each level 0 classifier

**for** train\_validation, test **in** STRATIFIEDKFOLD(data, n\_folds=6) **do**

    lstms = TRAINLSTMS(train\_validation)

    lstm\_probs = MEAN({PREDICT(lstm, test) | lstm  $\in$  lstms})

    xgb = TRAINXGB(train\_validation)

    xgb\_probs = PREDICT(xgb, test)

    metafeatures = metafeatures  $\cup$  CONCATENATE(lstm\_probs, xgb\_probs)

**end for**

stacking\_classifier = TRAINLDA(metafeatures)

xgb = TRAINXGB(data)

$\triangleright$  Train the level 0 classifiers with all data

lstms = TRAINLSTMS(data)

**OUTPUT:** xgb, lstms, stacking\_classifier

---

**Table 5:** Example of stratified 8-fold cross-validation

Method	Fold Number								Mean (SD)
	0	1	2	3	4	5	6	7	
XGBoost	0.889	0.874	0.862	0.866	0.871	0.905	0.908	0.867	0.880 (0.018)
LSTMs	0.866	0.868	0.849	0.862	0.848	0.870	0.886	0.862	0.864 (0.012)
LDA-stacker	0.904	0.883	0.872	0.887	0.872	0.901	0.905	0.886	0.889 (0.013)

**Table 6:** Per-class performance in training and test sets

	Training set cross-validation mean $F_1$ (SD)			Test set $F_1$	
	XGBoost	LSTMs	LDA-stacker	LDA-stacker	
				Official phase	Follow-up
<b>N</b>	0.953 (0.007)	0.955 (0.006)	0.960 (0.007)	0.90	0.92
<b>A</b>	0.838 (0.032)	0.796 (0.028)	0.842 (0.021)	0.85	0.86
<b>O</b>	0.850 (0.019)	0.841 (0.012)	0.864 (0.019)	0.74	0.77
$\sim$	0.711 (0.063)	0.658 (0.052)	0.724 (0.045)	-	-
<b>Overall</b>	<b>0.880 (0.018)</b>	<b>0.864 (0.012)</b>	<b>0.889 (0.013)</b>	<b>0.83</b>	<b>0.85</b>

#### 4. Discussion and conclusions

The inconsistency problems in the Challenge dataset suggest that giving complete independence to human experts leads to a high level of disagreement in the resulting labels, even in a relatively bounded and well-defined problem from the clinical perspective like the ECG arrhythmia classification. However, the presence/absence of diseases like atrial fibrillation is not a subjective consideration, and medical guidelines prove that consensus can be achieved (Camm, Kirchhof, Lip et al. 2010). We defend that such a consensus should be the first step for the development of an effective low-

cost screening system, as it removes the need for dozens of experts and thousands of records to achieve an statistically acceptable agreement, while allowing for less complex algorithms. We would like to point out that by “consensus” we are not referring to a strong quantification of decision thresholds, but to general guidelines shared by the expert labelers. A possible example could be: “*Atrial flutters will be considered in the  $O$  class*”, which reduces the probability of inconsistencies such as the one in Figure 5b.

Having these guidelines, and on the basis of the achieved results in the Challenge, we consider that a reduced set of two or three experts and some hundreds of records should be enough to achieve a much higher performance of the classification algorithm, with an  $F_1$  over 0.9. Additionally, it would be desirable that labeling would be made on standard multi-lead ECG records acquired simultaneously to the single-lead record, to quantify the information loss of the handheld device for this specific problem. We expect to conduct this study in the near future.

The interpretation of ECG signals is a task in which humans show an outstanding proficiency. But even if qualities like personal experience or intuition are invaluable and hardly formalizable, the pathophysiological processes that can be observed in the ECG and the effects they have on the signal behavior are widely accepted in the medical community. Also, systematic approaches such as those described in ECG handbooks (Wagner 2008) provide excellent results for screening and diagnosis, and most of that expert knowledge is susceptible of being formalized by computational methods.

The official results of the Challenge show that all best-performing algorithms include domain-specific knowledge at some point. This suggest that knowledge-based approaches have a fundamental advantage over pure learning-based approaches in quantifying the underlying criteria of manually labeled datasets. In the present proposal, we demonstrated that exploiting this advantage is feasible without sacrificing the benefits of sophisticated machine learning methods and maintaining a notable degree of interpretability by the use of meaningful features.

Finally, in this Challenge the *Construe* algorithm has reaffirmed its ability to accurately interpret highly contaminated data by combining bottom-up reasoning (guided by data) and top-down reasoning (guided by knowledge) in an abductive cycle. As forthcoming work, the integration of new signal types beyond the ECG, such as for example the blood pressure, has the potential to further improve the robustness and the accuracy of the results.

## Acknowledgements

This work was supported by the Spanish Ministry of Economy and Competitiveness under project TIN2014-55183-R. C.A. García is also supported by the FPU Grant program from the Spanish Ministry of Education (MEC) (Ref. FPU14/02489). We would also like to acknowledge Alberto Cobos for his work on the lead inversion detection problem during his CiTIUS summer fellowship 2017, and the Challenge organizing team for the great support and encouragement given to the competitors at all times.

## References

- Bergstra, J., Yamins, D. & Cox, D. (2013). Making a science of model search: Hyperparameter optimization in hundreds of dimensions for vision architectures, *International Conference on Machine Learning*, pp. 115–123.
- Camm, A. J., Kirchhof, P., Lip et al. (2010). Guidelines for the management of atrial fibrillation: the Task Force for the Management of Atrial Fibrillation of the European Society of Cardiology (ESC)., *European heart journal* **31**(19): 2369–429.
- Caruana, R., Lou, Y., Gehrke, J., Koch, P., Sturm, M. & Elhadad, N. (2015). Intelligible Models for HealthCare, *21th ACM SIGKDD International Conference on Knowledge Discovery and Data Mining*.
- Chen, T. & Guestrin, C. (2016). XGBoost: A Scalable Tree Boosting System, *22nd ACM SIGKDD International Conference on Knowledge Discovery and Data Mining*.
- Chollet, F. et al. (2015). Keras, <https://github.com/keras-team/keras>.
- Clifford, G., Liu, C., Moody, B., Lehman, L., Silva, I., Li, Q., Johnson, A. & Mark, R. (2017). AF classification from a short single lead ECG recording: The Physionet Computing in Cardiology Challenge 2017, *Computing in Cardiology*.
- Glorot, X., Bordes, A. & Bengio, Y. (2011). Deep sparse rectifier neural networks, *Proceedings of the Fourteenth International Conference on Artificial Intelligence and Statistics*, pp. 315–323.
- Goldberger, A. et al. (2000). PhysioBank, PhysioToolkit and PhysioNet: Components of a New Research Resource for Complex Physiologic Signals, *Circulation* **101**: 215–220.
- Guyon, I., Weston, J., Barnhill, S. & Vapnik, V. (2002). Gene selection for cancer classification using support vector machines, *Machine Learning* **46**(1-3): 389–422.
- Kingma, D. & Ba, J. (2014). Adam: A method for stochastic optimization, *arXiv preprint arXiv:1412.6980*.
- Pedregosa, F., Varoquaux, G., Gramfort, A., Michel, V., Thirion, B., Grisel, O., Blondel, M., Prettenhofer, P., Weiss, R., Dubourg, V., Vanderplas, J., Passos, A., Cournapeau, D., Brucher, M., Perrot, M. & Duchesnay, E. (2011). Scikit-learn: Machine Learning in Python, *Journal of Machine Learning Research* **12**: 2825–2830.
- Petrénas, A., Marozas, V. & Sörnmo, L. (2015). Low-complexity detection of atrial fibrillation in continuous long-term monitoring., *Computers in biology and medicine* **65**: 184–91.
- Sörnmo, L. & Laguna, P. (2005). *Bioelectrical Signal Processing in Cardiac and Neurological Applications*, Elsevier Academic Press.
- Srivastava, N., Hinton, G. E., Krizhevsky, A., Sutskever, I. & Salakhutdinov, R. (2014). Dropout: a simple way to prevent neural networks from overfitting., *Journal of machine learning research* **15**(1): 1929–1958.
- Teijeiro, T., Félix, P. & Presedo, J. (2015). A noise robust QRS delineation method based on path simplification, *2015 Computing in Cardiology Conference (CinC)*, pp. 209–212.
- Teijeiro, T., Félix, P., Presedo, J. & Castro, D. (2016). Heartbeat classification using abstract features from the abductive interpretation of the ECG, *IEEE Journal of Biomedical and Health Informatics*.
- Teijeiro, T., García, C. A., Castro, D. & Félix, P. (2017). Arrhythmia Classification from the Abductive Interpretation of Short Single-Lead ECG Records, *Computing in Cardiology*, Vol. arXiv preprint 1711.03892.
- Wagner, G. S. (2008). *Marriott's Practical Electrocardiography*, 11 edn, Wolters Kluwer Health/Lippincott Williams & Wilkins.
- Wolpert, D. H. (1992). Stacked generalization, *Neural networks* **5**(2): 241–259.